

## Phase diagram of uranium at high pressures and temperatures

Choong-Shik Yoo, Hyunchoe Cynn, and Per Söderlind

*H-Division, Physics and Space Technology Directorate, Lawrence Livermore National Laboratory, Livermore, California 94551*

(Received 3 November 1997)

The phase diagram of uranium has been studied to 100 GPa by *in situ* diamond-anvil cell x-ray/laser-heating experiments. The  $\gamma$  (bcc) phase is discovered at high pressures, and the melting curve is presented to 100 GPa. The  $\gamma$  phase,  $B=113.3$  GPa, is approximately 20% softer than the  $\alpha$  (orthorhombic),  $B=135.5$  GPa. The volume change in the  $\alpha/\gamma$  transition shows a strong pressure dependence, ranging from 6% at ambient pressure to less than 1% at 80 GPa. Free-energy calculations, using Debye-Grüneisen quasiharmonic theory, show that the softer bulk modulus of the  $\gamma$  phase, compared to the  $\alpha$  phase, stabilizes the  $\gamma$  phase at high temperatures. [S0163-1829(98)10817-2]

The light actinides (Th-Pu) exhibit a profound polymorphism of the crystal structures<sup>1</sup> and at ambient condition they (except for Th) solidify in exotic structures not found elsewhere in the periodic table. During the last few years an understanding of this behavior has emerged; the distorted crystal structures in the actinides originate from very narrow  $5f$  bands situated close to the Fermi level.<sup>2</sup> As we proceed through the series of the actinides, two distinct parts of the series are discovered. The early part, from Th-Pu, shows a parabolic behavior of the equilibrium volume, bulk modulus, and cohesive energy, reminiscent of the  $d$ -transition metals, whereas the later part shows a more constant behavior of these properties as a function of atomic number. The similarity between the light actinides and the  $d$ -transition metals in this regard is governed by the fact that the light actinides and the  $d$ -transition metals both have delocalized electrons,  $f$  and  $d$ , respectively.<sup>3,4</sup> For the heavier actinides from americium and on, however, the  $5f$  electrons are localized similar to the lanthanide series and their properties become quite different from that of the earlier actinides. The itinerant  $5f$  electrons also show a distinguished difference compared to the  $4d$  and  $5d$  electrons, namely, their bandwidths are much narrower and in turn this leads to Peierls distortion of the crystal structures of the light actinides.<sup>2</sup> At high compression the heavier actinides are expected to also attain distorted crystal structures because of pressure-induced delocalization of  $5f$  electrons.<sup>5,6</sup>

Uranium, with a central position in the early actinide series, crystallizes into a rather open structure, the orthorhombic  $\alpha$ -phase with four molecules per unit cell at ambient condition.<sup>1</sup>  $\alpha$ -U is unique in that it remains stable up to at least 100 GPa at ambient temperature<sup>7,8</sup> whereas the other light actinides undergo phase transition below this pressure. The  $\alpha$  phase transforms to the body-centered tetragonal  $\beta$ (bct) phase at 940 K (Ref. 9) and then to the  $\gamma$  (bcc)-phase at 1050 K at ambient pressure.<sup>10</sup> The  $\alpha/\beta$ - and  $\beta/\gamma$ -phase boundaries were measured previously to 5 GPa by resistivity measurements, with the  $\alpha/\beta/\gamma$ -triple point at 3 GPa.<sup>11</sup> The melting temperatures of uranium have been determined to 45 GPa by laser-heating experiments and also calculated to 100 GPa by generalized pseudopotential theory.<sup>12</sup> The bcc structure has often been assumed for the phase of uranium at high pressures and temperatures in both previous resistivity

measurements,<sup>11</sup> and calculations,<sup>12</sup> although it has never been observed experimentally.

In this paper, we report the structural investigation of  $\gamma$ (bcc)-U in a wide range of pressures and temperatures by *in situ* x-ray diffraction of laser-heated uranium in a diamond-anvil cell. The phase diagram of uranium is presented to 100 GPa and 4500 K, together with various thermal properties of uranium including thermal expansibility, equation of state (EOS), transition volume changes, and extended melting temperatures. These experimental results are then complemented with first-principles theory, which mainly focus upon the stability of the  $\gamma$  compared to the  $\alpha$  phase of uranium.

A small piece of thin uranium foil, ( $\sim 10$   $\mu\text{m}$  thick,  $\sim 30$  to 50  $\mu\text{m}$  square in size) was loaded in a diamond-anvil cell of the Mao-Bell type, together with a pressure medium such as Ar and  $\text{Al}_2\text{O}_3$ , and Ruby crystals. Ar was typically used for the experiments below 40 GPa and  $\text{Al}_2\text{O}_3$  for higher pressures; no difference in results was observed from these pressure media. Using a YLF laser (25 W at TEM<sub>00</sub>, coherent), the sample was heated in a small step and the temperature was determined in each step by thermal emission measured at the center of laser-heated area. The melting was then characterized visually by diffusive motion of the sample, forming a microchannel and/or altering the shape at the edge. The melting temperatures at several pressures were also compared with those determined by *in situ* x-ray diffraction described below, showing a good agreement within the experimental uncertainties of two methods. The details of the melting experiments have been discussed previously.<sup>12</sup>

A white x-ray beam from the synchrotron is coaxially aligned to the center of laser-heated area and then the x-ray diffraction from the sample is recorded at a fixed  $2\Theta$  angle as a function of energy to determine the crystal structure.<sup>13,14</sup> The temperature is determined simultaneously with the x-ray measurement, again by the thermal emission and the pressure is determined either from the EOS of the sample or by the Ruby luminescence method. The x-ray beam size,  $10 \times 10$   $\mu\text{m}$ , is comparable to the size of laser-heating spot that varies from 30 to 100  $\mu\text{m}$  depending on temperature. Therefore, there could be large temperature gradients in both the radial and axial directions of the sample being x rayed; we estimate the temperature gradients could be as much as 10%

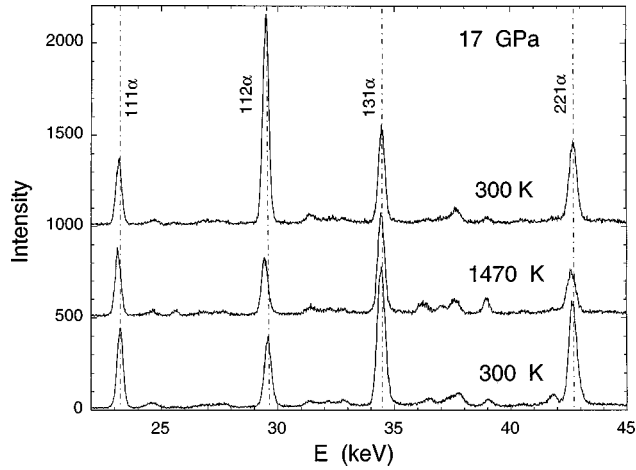


FIG. 1. Energy dispersive x-ray diffraction of  $\alpha$ (orthorhombic)-U obtained before (300 K, bottom spectrum), during (1470 K, middle), and after (300 K, top) laser heatings at 17 GPa.  $Ed = 51.163 \text{ keV \AA}$ .

of the value reported here. The x-ray diffraction was collected at  $2\Theta$  between  $14^\circ$  and  $21^\circ$  for 1–10 min to obtain the spectra presented here.

Figure 1 represents a typical change of the diffraction pattern during laser-heating experiments. Apparently all the reflections shift to lower energy (or higher  $d$  spacing) during heating, which occurs reversibly during heating cycles. The diffraction patterns are well indexed to the  $\alpha$ (orthorhombic) phase of uranium, resulting in the volumes of  $11.368 \text{ cm}^3/\text{mol}$  before heating,  $11.457 \text{ cm}^3/\text{mol}$  during heating at 1470 K, and  $11.405 \text{ cm}^3/\text{mol}$  after a few successive heating cycles. The reversibility of the volume during the heating cycles is better than 0.3% in volume or 1 GPa in pressure, well within the uncertainty of measurements. The volume expansion coefficient  $\alpha_v = 5.3 (\pm 1.5) \times 10^{-6} \text{ K}^{-1}$  at 17 GPa is substantially smaller than that at ambient condition,  $39 \times 10^{-6} \text{ K}^{-1}$ ,<sup>6</sup> but is typical for those of corresponding 4d- or 5d-transition metals.<sup>15</sup> It is also apparent from Fig. 1 that the 131 reflection shifts little with respect to other

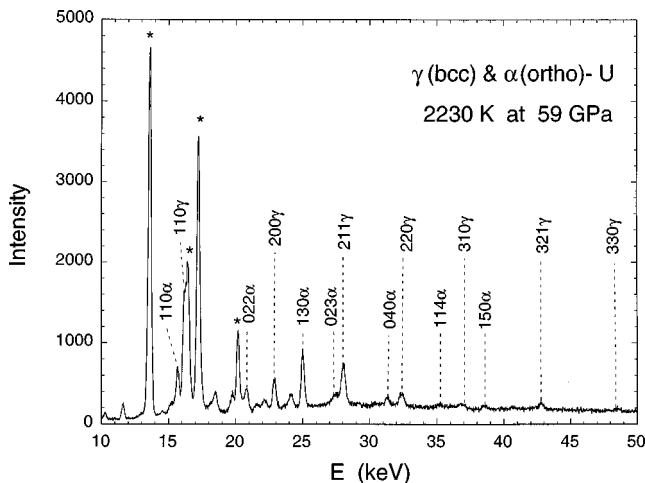


FIG. 2. Energy dispersive x-ray diffraction of the  $\alpha/\gamma$ -mixture near the onset of the  $\alpha \rightarrow \gamma$  transition at 59 GPa and 2230 K (see Table I). The peaks with asterisks are the fluorescence lines of uranium.  $Ed = 36.610 \text{ keV \AA}$ .

TABLE I. The  $\gamma$ (bcc) phase of uranium near the onset of  $\alpha/\gamma$  transition at 59 GPa and 2230 K (see Fig. 2).  $\gamma$  (bcc)-U:  $a = 3.198 \text{ \AA}$ ,  $V = 9.872 \text{ cm}^3/\text{mol}$ .  $\alpha$  (orthorhombic)-U:  $a = 2.606 \text{ \AA}$ ,  $b = 5.308 \text{ \AA}$ ,  $c = 4.663 \text{ \AA}$ ,  $V = 9.737 \text{ cm}^3/\text{mol}$ ,  $\Delta V_T = 1.39\%$ .

$hkl$	$E_{\text{obs}}$	$d_{\text{obs}}$	$I_{\text{obs}}$	$d_{\text{calc}}$	$I_{\text{calc}}$	$\Delta d_{\text{obs-calc}}$
110	16.179	2.263	100.0	2.261	100.0	0.002
200	22.895	1.599	19.8	1.599	24.0	0.000
211	28.044	1.305	27.3	1.305	35.0	0.000
220	32.387	1.130	10.5	1.131	6.4	-0.001
310	36.137	1.013	3.4	1.011	4.9	0.002
321	42.826	0.855	6.7	0.855	1.8	0.000
330	48.602	0.753	4.6	0.754	1.0	-0.001

reflections, suggesting large anisotropy in thermal expansion. The linear thermal expansion coefficient for the  $b$  axis, the largest axis of the unit cell, is about  $\alpha_L = 1.1 \times 10^{-6} \text{ K}^{-1}$  and for the  $a$  and  $c$  axes  $3.0 \times 10^{-6} \text{ K}^{-1}$  and  $3.6 \times 10^{-6} \text{ K}^{-1}$ , respectively. A similar anisotropy of  $\alpha$ -U was observed in the previous compression experiments at ambient temperature.<sup>8</sup>

At higher temperatures the  $\alpha$ -phase transforms into the  $\gamma$ (bcc) phase. Figure 2 is a typical diffraction pattern near the onset of the transition at 59 GPa. All the major peaks are well indexed to a mixture of the  $\gamma$  and  $\alpha$  phases (Table I). The volume of  $\gamma$ -U,  $9.872 \text{ cm}^3/\text{mol}$ , is approximately 1.39% larger than that of  $\alpha$ -U,  $9.737 \text{ cm}^3/\text{mol}$ . The volume change in the transition is strongly dependent on pressure, as illustrated in Fig. 3. It decreases from approximately  $0.8 \text{ cm}^3/\text{mol}$  ( $\Delta V_T/V_\alpha = 5.94\%$ ) at ambient pressures to less than  $0.1 \text{ cm}^3/\text{mol}$  (0.74%) at 80 GPa.

The pressure-volume relation of  $\gamma$ -U is illustrated in Fig. 4. The volumes for  $\gamma$ -U were determined at different temperatures between 1300 and 2000 K. However, considering a substantially smaller volume change by temperature than by pressure, we use a temperature independent Birch-

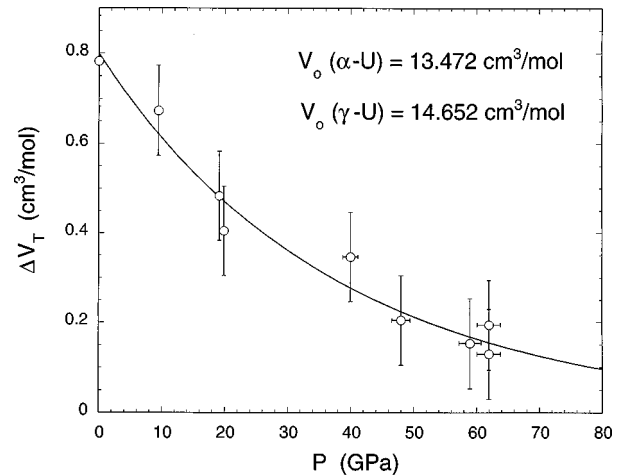


FIG. 3. The volume change in  $\alpha$ - $\gamma$  transitions  $\Delta V_T$  as a function of pressure.  $\Delta V_T$  values were calculated from the x-ray diffraction(s) obtained near the onset of transition or at two nearest temperatures at a given pressure. The temperature-induced volume change in the later case is estimated less than  $0.5 \text{ cm}^3/\text{mol}$ , well within the uncertainty of measurements.

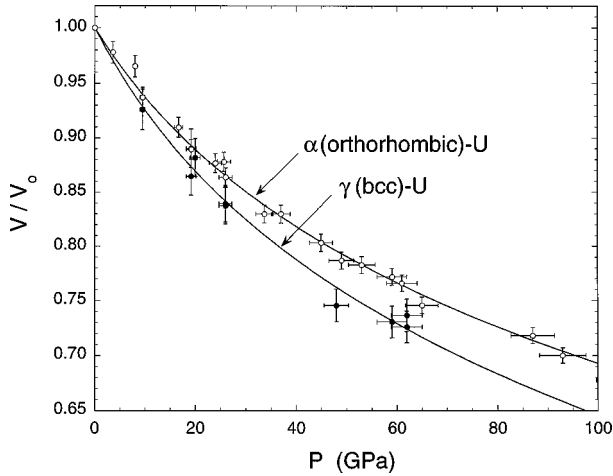


FIG. 4. Volume compression data of  $\gamma$ - (solid circles) and  $\alpha$ -U (open circles) and the fits to a temperature-independent Birch-Murnaghan equation of state. The fits result in  $B=135.5$  GPa and  $B'=3.79$  for  $\alpha$ -U and  $B=113.3$  GPa and  $B'=3.37$  for  $\gamma$ -U.

Murnaghan equation of state<sup>16</sup> to fit the data with  $B=135.5$  GPa and  $B'=3.8$  for  $\alpha$ -U and  $B=113.3$  GPa and  $B'=3.4$  for  $\gamma$ -U. The data for  $\alpha$ -U are in agreement with those reported previously.<sup>7</sup> Note that  $\gamma$ -U has a softer (20%) bulk modulus and we shall see the importance of this in stabilizing this phase at higher temperatures.

The melting temperatures of uranium have been extended to 100 GPa from our previous results,<sup>12</sup> as shown in Fig. 5. The melting temperatures of these and previous studies have been determined primarily by visual observation (open circles), but at several pressures by *in situ* x-ray diffraction (solid circles). Both sets of data agree within the uncertainty of measurements. The crystal structure of uranium as determined by *in situ* x-ray diffraction is also illustrated for  $\gamma$ -U (solid squares), but not for the  $\alpha$  phase for simplicity. The  $\alpha/\gamma$  phase boundary is drawn below the stability field of  $\gamma$ -U and is constrained at the transition temperature of the  $\alpha$  phase, 940 K, at ambient pressure. This interpolation results in a relatively strong curvature of the  $\alpha/\gamma$ -phase boundary at

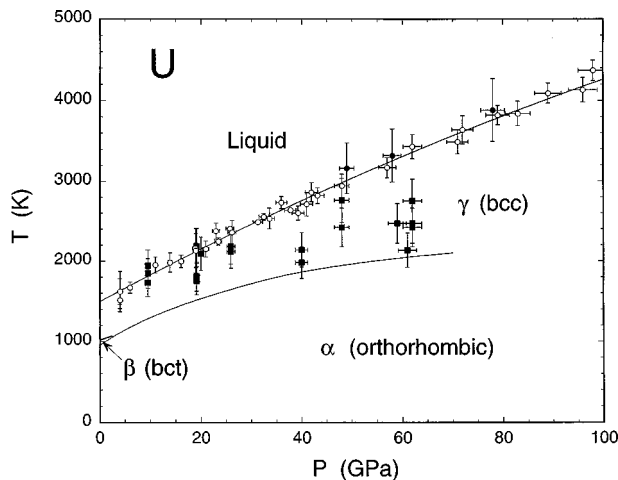


FIG. 5. Phase diagram of uranium to 100 GPa. Open and solid circles, respectively, indicate the melting temperatures determined by visible observation and x-ray diffraction. The solid squares represent the  $P, T$  conditions at which  $\gamma$ (bcc)-U was *in situ* observed.

low pressures, which is consistent with a strong pressure dependence in the transition volume change (Fig. 3). Note that the slope of the  $\alpha/\gamma$ -phase line becomes diminishingly small above 70–80 GPa and the  $\gamma$  phase occupies a large stability field at high pressures and temperatures. The stability field of  $\beta$ (bct)-U below 3 GPa is also reproduced from the previous measurements.<sup>11</sup>

First-principles treatment of actinides at high temperatures is rather challenging; whereas, *ab initio* full potential electronic structure calculations<sup>2</sup> of the bcc structure at low temperature result in rather poor descriptions of  $B=180$  GPa,  $B'=4.2$ , a smaller equilibrium volume than  $\alpha$ -U, and a negative tetragonal shear constant  $C'$  at 100 GPa. Hence, our zero-temperature theory fails to describe  $\gamma$ -U at high temperatures, although it describes  $\alpha$ -U rather well. In order to clarify the occurrence of the bcc phase at high temperatures, we made a series of free-energy calculations using Debye-Grüneisen quasiharmonic theory.<sup>6</sup> In these calculations, we also include temperature dependence of the electronic structure and calculate the Helmholtz free energy as

$$F(V, T) = E_{\text{el}}(V, T) + E_{\text{ph}}(V, T) - T[S_{\text{ph}}(V, T) + S_{\text{el}}(V, T)]. \quad (1)$$

Here all terms depend upon volume and temperature and the electronic contributions  $E_{\text{el}}(V, T)$  and  $S_{\text{el}}(V, T)$  were obtained from our first-principles calculations where  $E_{\text{el}}$  is the total energy calculated with a temperature broadening (Fermi-Dirac distribution) of the density of states and  $S_{\text{el}}$  the electronic entropy as obtained from Landau and Lifshitz.<sup>17</sup> The other terms are described in detail elsewhere.<sup>8,18</sup> We calculated the Helmholtz free energy, using Eq. (1), for  $\alpha$ -U and  $\gamma$ -U; at zero temperature the difference in free energy is to be about 10 mRy but at 3000 K the free-energy difference has decreased to about half of this value. Most of this lowering of the bcc energy was due to the electronic contributions. The other terms in the free energy showed a very similar temperature dependence for the two phases. Their Debye temperatures at room temperature were very close ( $\gamma$ -U: 270 K and  $\alpha$ -U: 280 K) and so were their thermal expansion coefficients ( $\gamma$ -U:  $\alpha_v = 24.6 \times 10^{-6} \text{ K}^{-1}$  and  $\alpha$ -U:  $\alpha_v = 26.8 \times 10^{-6} \text{ K}^{-1}$ ). In the Debye-Grüneisen quasiharmonic theory the Debye temperature is obtained directly from the bulk modulus and consequently this property is of essential importance for calculating the free energy in this model. Therefore, in a model calculation, we replaced the computed bulk modulus for bcc U with the experimental value, without changing any other parameters from our first-principles calculation. At room temperature we now instead obtained the Debye temperature 229 K and thermal expansion coefficient  $\alpha_v = 39 \times 10^{-6} \text{ K}^{-1}$ . More importantly, at 2500 K the free energy of this model phase became lower than that of  $\alpha$ -U, indicating a possibility for this phase to be stabilized at higher temperatures.

We consider the localization effects of  $5f$  electrons to explain the high-temperature behavior of  $\gamma$ -U, similar to the case of  $\delta$ -Pu.<sup>19</sup> A complete localization is rather straightforward to simulate in a calculation by forcing the  $5f$  electrons to fill core states of the U atoms. This however results in a too large equilibrium volume with a too low bulk modulus and pressure derivative ( $B=50$  GPa and  $B'=1.4$ ). Clearly, a full localization of the  $5f$  electrons does not reproduce ex-

perimental findings. Therefore, it is more likely that the  $5f$  electrons are partially localized; this would then be consistent with a lower bulk modulus for  $\gamma$ -U and a 6% volume increase at the transition from  $\alpha$ -U to  $\gamma$ -U. The transitions of  $\alpha$ -U to  $\beta$ (bct) and  $\gamma$ (bcc), at ambient pressure support this conclusion because bct is the ground-state crystal structure of Pa, the metal preceding U with one less delocalized  $5f$  electron.

In summary, we have discovered the  $\gamma$ (bcc) phase of uranium at high pressures and presented the phase diagram of uranium to 100 GPa. Our results indicate (i) a small thermal expansion coefficient of uranium at high pressure, (ii) a strong pressure dependence of the  $\alpha/\gamma$  transition volume change, (iii) softening of the  $\gamma$  phase of uranium at high temperatures, (iv) a wide stability field of the  $\gamma$  phase at high pressures and temperatures. Based on these results and free-energy calculations, we conjecture that the  $\gamma$  phase is induced by partial localization of the  $5f$  electrons at high temperatures. On the other hand, the bcc structure has been

considered as the ultimate phase of the light actinides at elevated pressures as a consequence of the increased importance of the Madelung (electrostatic) energy, driving the metal to close-packed high symmetry structures, and decreased importance of the Peierls distortion for broader bands (stabilizing distorted structures).<sup>2</sup> In this regard, it would be very interesting to see how these two bcc phases from different physical origins can merge at very high pressures and temperatures.

The x-ray studies were done at the beamline X17C of the NSLS and technical support of NSLS, particularly from Jingzhu Hu is appreciated. We also thank J. A. Moriarty and A. McMahan for highly valuable discussions, and L. Wiley, B. Goodwin, and C. Mailhot for the programmatic support. This work was performed under the auspices of the U.S. Department of Energy by the Lawrence Livermore National Laboratory under Contract No. W-7405-ENG-48.

- 
- <sup>1</sup>D. A. Young, *Phase Diagrams of the Elements* (University of California Press, Berkeley, CA, 1991), Chap. 15, p. 221.
- <sup>2</sup>P. Söderlind, O. Eriksson, B. Johansson, J. M. Wills, and A. M. Boring, *Nature* (London) **374**, 524 (1995).
- <sup>3</sup>B. Johansson, *Phys. Rev. B* **11**, 2740 (1975).
- <sup>4</sup>A. K. McMahan, *J. Less-Common Met.* **149**, 1 (1989).
- <sup>5</sup>U. Benedict, *J. Phys. (Paris), Colloq.* **45**, C8 (1984).
- <sup>6</sup>P. Söderlind, L. Nordström, L. Yongming, and B. Johansson, *Phys. Rev. B* **42**, 4544 (1990).
- <sup>7</sup>J. Akella, G. S. Smith, R. Grover, Y. Wu, and S. Martin, *High Press. Res.* **2**, 295 (1990).
- <sup>8</sup>J. Akella, S. Weir, J. M. Wills, and P. Söderlind, *J. Phys.: Condens. Matter* **9**, L549 (1997).
- <sup>9</sup>J. Donohue, *The Structure of the Elements* (Wiley, New York, 1974), Chap. 5.
- <sup>10</sup>R. W. G. Wyckoff, *Crystal Structures* (Wiley, New York, 1963), p. 16.
- <sup>11</sup>W. Klement, Jr., A. Jayaraman, and G. C. Kennedy, *Phys. Rev.* **129**, 1971 (1963).
- <sup>12</sup>C. S. Yoo, J. Akella, and J. A. Moriarty, *Phys. Rev. B* **48**, 15 529 (1993).
- <sup>13</sup>C. S. Yoo, J. Akella, A. Campbell, H. K. Mao, and R. J. Hemley, *Science* **270**, 1473 (1995).
- <sup>14</sup>C. S. Yoo, P. Söderlind, J. A. Moriarty, and A. J. Campbell, *Phys. Lett. A* **214**, 65 (1996).
- <sup>15</sup>K. A. Gschneider, Jr., *Solid State Physics* (Academic, New York, 1964), Vol. 16, p. 275.
- <sup>16</sup>F. Birch, *J. Geophys. Res.* **57**, 227 (1952); *J. Appl. Phys.* **9**, 279 (1938).
- <sup>17</sup>L. D. Landua and E. M. Lifshitz, *Statistical Physics* (Pergamon, London, 1959).
- <sup>18</sup>V. L. Moruzzi, J. F. Janak, and K. Schwarz, *Phys. Rev. B* **37**, 790 (1988).
- <sup>19</sup>O. Eriksson and J. M. Wills (unpublished).